Kinetic Simulations of Fast Ion in Stellarators

A. Bustos[1,2], F. Castejón[1,2], M. Osakabe[3],
L. A. Fernández[2,4], V. Martin-Mayor[2,4]

[1] National Fusion Laboratory, EURATOM-CIEMAT, 28040 Madrid, Spain
[2] BIFI, Zaragoza, Spain
[3] National Institute for Fusion Science,322-6 Oroshi-cho, Toki 509-5292, Japan
[4] Complutense University, Madrid, Spain
Email: andres.debustos@ciemat.es
Keywords:Fast particles, confinement studies, stellarator.

Abstract

The steady state distribution function of NBI fast ions is calculated numerically for the LHD and TJ-II stellarators using the code ISDEP (Integrator of Stochastic Differential Equations for Plasmas). ISDEP is an orbit code that solves the guiding center motion of fast ions using Cartesian coordinates in position space, allowing arbitrary magnetic configurations and the reentering of particles in the plasma. It takes into account collisions of fast ions with thermal ions and electrons using the Boozer and Kuo-Petravic collision operator. The steady state distribution function is computed with a time integral following Green's function formalism for a time independent source. The rotation profiles of the fast ions are also estimated, thus computing their contribution to the total plasma current. In addition, energy slowing down time and escape distribution are studied in detail for both devices.

1 Introduction

Neutral Beam Injection (NBI) heating plays a crucial role in the physics of most fusion devices, since it is a valuable method for plasma heating and fueling and could be very useful for driving current and momentum. In the present work, the NBI fast ion distribution function is calculated numerically for LHD and TJ-II [1] plasmas using the orbit code ISDEP (Integrator of Stochastic Differential Equations for Plasmas) [2]. The steady state distribution function is calculated using Green's function formalism.

The fast ion population is considered as a perturbation to a static plasma background and its dynamics given by the guiding center motion and collisions with thermal ions and electrons. Even thought fast ions are in the low collisionality regime, the complexity of the magnetic field in 3D devices implies that a numerical solution of the fast ion transport is mandatory. ISDEP is an orbit Monte Carlo code that solves the Fokker-Planck equation for the test particle population integrating ion guiding center equations of motion in the 5D phase space: (x, y, z, v^2, λ). The Boozer-Kuo Petravic collision operator for ion-ion and ion-electron collisions with the background plasma is implemented in ISDEP. The code

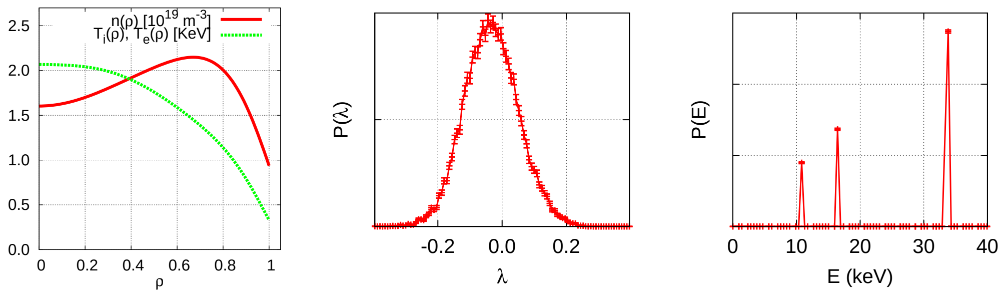

Figure 1: Density and ion and electron temperature profiles used in the simulations for LHD (left), provided by VMEC, in the standard configuration with $R_0 = 3.60$. The fast ion initial distribution is given by HFREYA. It is centered in 0 in the pitch (center) and presents three peaks in the energy (right).

avoids approximations on the size of the orbits and on the diffusive nature of transport. ISDEP uses Cartesian coordinates, allowing to include geometries with magnetic islands or ergodic zones as well as the scrape-off-layer volume where the field lines are open. As a consequence, the properties of ion transport in the whole device can be studied as well as the hit points of escaping ions on the vacuum chamber, as was done in Ref. [3] for TJ-II. These collisions with the vacuum vessel are the only test particle losses in this work since reentering particles are taken into account. The equations of motion and details about the code can be found in [2]. On the other hand, ISDEP usually requires more CPU time than magnetic coordinates-based codes since the equations of motion in Cartesian coordinates are much more complicated.

The steady state distribution function is calculated for a stationary source. This is a good approximation for the NBI heating in which the injectors launch an almost constant current of neutrals with constant energy spectrum. In this work two different situations are considered: perpendicular beam injection for LHD and tangential injection for TJ-II. Comparison with experimental data will be done in future works.

2 Plasma and initial Conditions

The plasma background equilibria in the two stellarators are obtained with VMEC considering the typical plasma profiles for this type of discharges. The scrape-off-layer profiles are estimated with an extrapolation of the equilibrium profiles. An exponential decay outside the plasma is assumed for density and temperature profiles, while the electric potential is kept constant.

Although in LHD most of the NBI heating power comes from tangential injection, in this work we simulate fast ions injected perpendicularly by NBI line number 4 (6 MW power). Line 4 is especially valuable for future comparisons with experimental data. The ions are initialized following the distribution function provided by the code HFREYA (Fig. 1). HFREYA is a Monte Carlo code that estimates the dynamics of fast neutrals inside the plasma, including propagation, ionisation and charge exchange. In the LHD simulations the electric field is neglected since it is too small to have consequences on the orbits of such fast ions. Fig. 1 also shows the plasma equilibrium profiles. TJ-II is equipped with two tangential injectors that launch neutrals in co and counter directions. We simulate

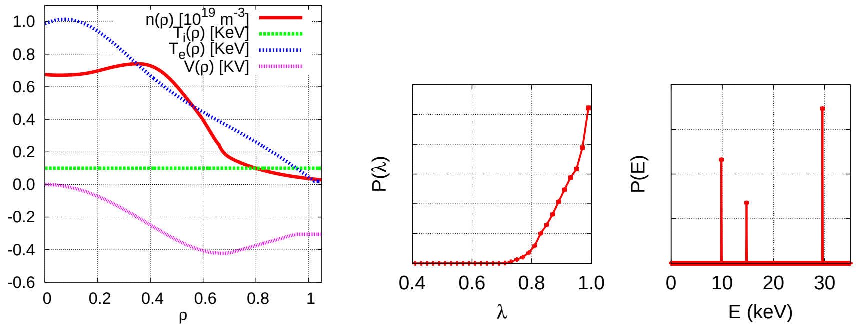

Figure 2: Same as Fig 1 for TJ-II.

here the neutrals injected tangentially with line number 1 (co-directed to the magnetic field). The birth point locations in phase space are estimated with FAFNER2, which is another Monte Carlo code similar to HFREYA. TJ-II simulations with ISDEP do take into account the electric field because it is not negligible in this case. Fig. 2 shows the plasma background profiles for the simulations as well as the energy and pitch angle distribution of the fast ions created from the fast neutrals. These conditions are representative of the initial phase of an NBI discharge.

3 Steady State Distribution Function

Many relevant properties of the fast ion confinement can be obtained taking statistical measurements on the trajectories of the launched particles. In this section we calculate a marginal distribution of the fast ion distribution function $f(t, x, y, z, v^2, \lambda)$. Position space is expressed by means of the effective radius ρ and velocity space in terms of the two components of the velocity $(v_{||}, v_{\perp})$. This 4D space is discretized with a 4 dimensional histogram in $(t, \rho, v_{||}, v_{\perp})$. Every trajectory contributes to f, increasing the statistics according to the initial state and single particle dynamics. Note that what is obtained with ISDEP is the distribution function multiplied by the jacobian: $f(t, \rho, v_{||}, v_{\perp}) \cdot J(\rho, v_{\perp})$. The steady state of this quantity is calculated with the Green function formalism, following [4].

It is important to remark that this approximation is valid as long as the plasma background is not modified and the number of test particles much smaller than the total number of particles in the plasma. When the bulk plasma heating and fueling are important, it losses its validity and we have to introduce a self-consistent model.

Except for a multiplicative constant, the distribution function is calculated by ISDEP after integrating $\sim 10^5$ test particle trajectories and analyzing the results. The equations of motion and the method used to analyze the set of trajectories can be found in [2]. Around $5 \cdot 10^4$ CPU-hours have been needed, provided by grid and high performance computing. The function $f(x, t)$ does not necessarily have to be a distribution function. It can be any other time dependent quantity of the fast ion population, as the average rotation and radial velocities (Section 4).

Due to its linear nature, ISDEP cannot provide absolute values of f, hence the results are presented normalized so that $\sum_{ijk} J(\rho_i, v_{\perp k}) f(\rho_i, v_{||j}, v_{\perp k}) = 1$ where the indexes i, j, k run

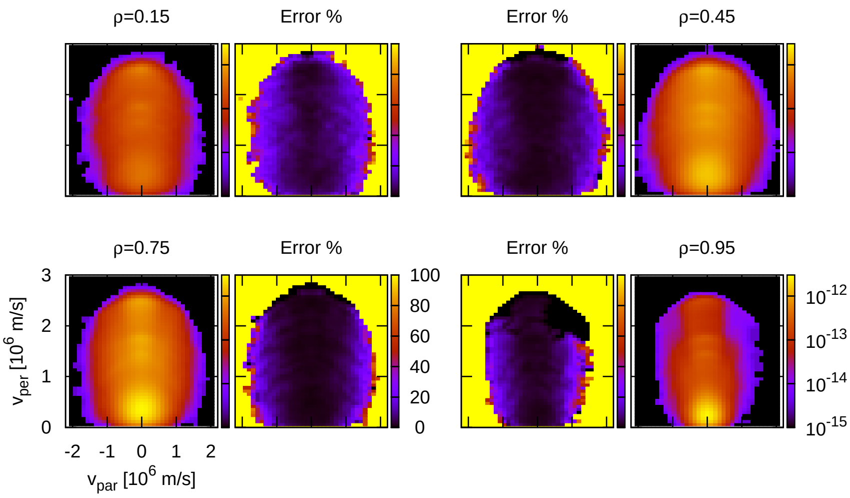

Figure 3: $J(\rho, v_\perp) \cdot f(\rho, v_{||}, v_\perp)$ and the relative error for four different radial positions in the steady state for LHD.

over the discretized phase space. Nevertheless, real values can be calculated multiplying f times the incoming flux of particles.

3.1 Application to LHD and TJ-II

The distribution function of the LHD fast ions calculated following the above shown procedure is plotted in Fig 3 for four radial positions: $\rho = 0.15$, $\rho = 0.45$, $\rho = 0.65$ and $\rho = 0.95$. The error calculation is done using the Jack-Knife technique. This method avoids over estimations of the statistical error of non linear functions of the sample. It is seen that the ions tend to thermalize and spread in velocity space almost symmetrically in $v_{||}$. Traces of the continuous injection of high energy ions can be seen at all positions.

In TJ-II the situation is different, as can be seen in Fig. 4. The birth points of test particles are located close to the magnetic axis due to the fact that the background plasma density is too low in the edge. Hence there are not many trajectories of fast ions in the outermost part of the plasma. The injection is tangential to the direction of $\mathbf{B}$, therefore there are not high negative parallel velocities in the distribution and almost all the fast particles appear for positive parallel velocities. A strong dispersion in the pitch angle appears due to the pitch angle scattering. The thermalization of particles is much less effective in TJ-II than in LHD, which makes the distribution function much farther from the Maxwellian than in the case of LHD. It is also necessary to consider the effects of transport: the fast ions that appear at outer positions of TJ-II come from the center of the plasma. Finally, the strong decrease of fast ion density observed at the outermost magnetic surfaces can be understood just considering the direct losses.

4 Fast ion dynamics: Rotation and Slowing Down Time

The study of the toroidal rotation is important because it has strong influence on the confinement and contributes significantly to the total plasma current, modifying then

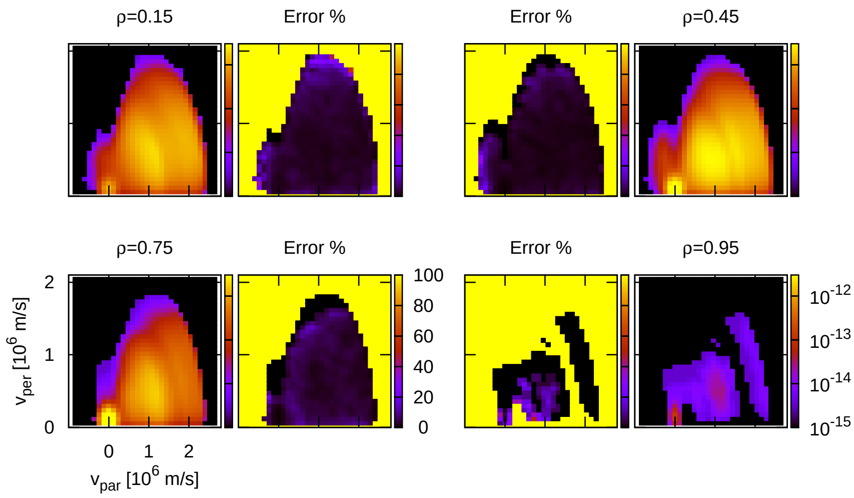

Figure 4: $J(\rho, v_\perp) \cdot f(\rho, v_{||}, v_\perp)$ for four different radial positions in the steady state for TJ-II.

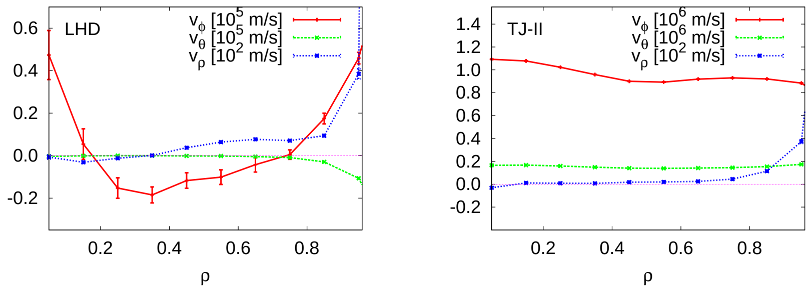

Figure 5: Toroidal and poloidal rotation and radial velocity profiles for LHD and TJ-II. The two fast ion population rotate in a different way due to the distinct initial conditions.

the confining magnetic field. Despite of the fact that the toroidal rotation is especially relevant in tokamaks, it is very useful to perform this study in a stellarator where the toroidal rotation is limited and the fast ions are the only momentum source, so it is possible to validate the presented models with experimental data.

Despite of the fact that the injection is almost perpendicular for LHD, the toroidal rotation (v_ϕ) is nonzero and presents a strong shear, changing sign twice while moving in the radial direction (Fig. 5). The mechanisms that determine this velocity are the initial conditions, the structure of the background magnetic field and the collisionality profiles, in a similar way as the bootstrap current is generated. The poloidal velocity v_θ is almost zero in most of the plasma column and becomes negative for $\rho > 0.8$. The radial velocity v_ρ, proportional to the outward particle fluxes, clearly presents three regions of interest. In the inner region of the plasma is zero or negative, meaning a very good confinement of fast ions. In the region defined by $0.4 < \rho < 0.8$, $v_\rho \sim 1\text{m/s}$ so the confinement gets worse. Near the border of the plasma where $\rho > 0.8$ the radial transport is higher, showing the effects of ion loses at these positions and a worse confinement of fast ions in the plasma edge.

In the case of TJ-II the results are quite different due to the different characteristics of the device and to the tangential injection. As expected, the average toroidal velocity of

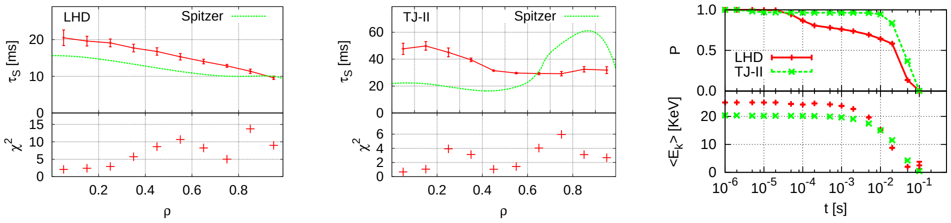

Figure 6: Slowing down time, calculated with a fit to Eq. 2 and with the Spitzer formula for LHD (left) and TJ-II (center). We plot the χ^2 for each fit. In these fits there are 14 degrees of freedom. The particle persistence and average energy as a function of time are also plotted (right).

the fast ions, v_ϕ, is much higher in TJ-II than in LHD, as can be seen in Fig. 5. In this case the high initial parallel velocity is so large that the influences of the structure of the magnetic field and the collisionality are not enough to reduce it substantially. The poloidal rotation v_θ is almost constant and the relative change of v_ρ along the radius is much smaller that in the LHD case, except in the plasma edge.

The slowing down time of the NBI ions is a very important quantity because it is related to the efficiency of the heating system. The shorter the slowing down time, the more efficient the power absorption by the plasma background and the more reduced the fast ion losses. It is defined as the time that the average energy of the beam takes to reach the background temperature. The energy slowing down time profile is calculated with the data of $f(t, \rho, v_{||}, v_\perp)$ from previous section. An integration gives the kinetic energy profile:

$$E(t, \rho) = \int \mathrm{d}v_{||}\,\mathrm{d}v_\perp J(\rho, v_\perp) f(t, \rho, v_{||}, v_\perp) \frac{m(v_{||}^2 + v_\perp^2)}{2}. \quad (1)$$

Assuming that the energy follows an exponential law in time, the slowing down time profile can be found with a fit to:

$$E(t, \rho) = A(\rho) + B(\rho)\mathrm{e}^{-\frac{t}{\tau(\rho)}}. \quad (2)$$

The slowing down time profile is plotted in Fig 6 for the two devices as well as the χ^2 of each fit with Eq. (2). In order to compare our results with the estimations of the neoclassical theory, we follow [5] to calculate the Spitzer slowing down time (see Fig. 6).

Discrepancies between the two time profiles can be observed in Fig. 6, being stronger for TJ-II than for LHD. These discrepancies can be understood by considering the effect of ion transport in the complex 3D geometry of the devices, especially of TJ-II, which is not taken into account in Spitzer formula. In the ISDEP calculation, the energy slowing down time is estimated including all the fast ion dynamics: transport, particle losses, geometrical features, apart from the collisional processes with thermal particles. In TJ-II these discrepancies with the theory are more important because the relation between the typical banana width and the minor radius is much higher than for LHD. Indeed this has consequences on transport and makes fast ions travel along a substantial fraction of the minor radius, making non-local effects relevant. The sudden increase of τ_S calculated with the Spitzer formula near $\rho = 0.6$ is due to the shape of the density and temperature profiles (Fig. 2), which present a strong gradient in that region.

Fig. 6 (right) shows the time evolution of the persistence of the fast ions. It is clearly seen that the curve cannot be fitted by an exponential, which means that the confinement

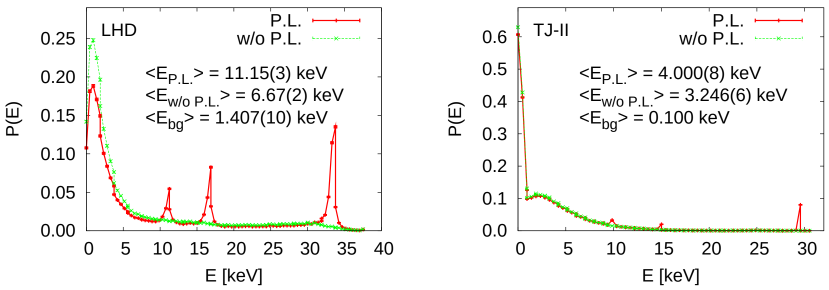

Figure 7: Energy distribution of losses for LHD and TJ-II. The energy spectra is plotted with and without considering prompt losses of the devices. The three peaks above 10 keV make prompt losses important in LHD. In TJ-II the peak near 30 keV is the only non negligible contribution to this effect.

presents a strong time dependence, showing two different time scales. The big slope in the persistence $P(t)$ at $t \sim 10^{-4}$ s for LHD is caused by prompt losses and corresponds to the first part of ion dynamics. Then a second phase appears, when ions suffer the slowing down process, which increases the bulk of the distribution function (as can be seen in Fig. 3). The average kinetic energy of confined ions is plotted in the same panel, showing that the prompt losses have not a strong effect in this quantity. For times $t > 10^{-2}$ s it is severely degraded when the majority of fast ions suffer the loss of confinement. Due to the different initial conditions (remind the tangential injection in TJ-II), prompt losses are much higher in LHD than in TJ-II. In fact, the former ones represent about 20% compared with 5% found in TJ-II .

The energy distribution of losses is plotted in Fig. 7. Two probability densities are calculated for each device: taking into account all escaping particles (with subscript P. L.) and removing the prompt losses (w/o P. L). In agreement with the former results, it is seen that the energy prompt losses are much more important for LHD. Moreover, the average energy of the lost particles is almost three times larger in LHD than for TJ-II.

5 Summary

The confinement properties of the NBI fast ions are studied for stellarators using the global Monte Carlo guiding center orbit code ISDEP. This code avoids common assumptions on the diffusive nature of transport and on the radial size of the ion orbits. It also allows to follow particles in the scrape off layer, therefore taking into account phenomena like the re-entrance of ions in the plasma. The steady state is estimated by using Green function techniques. The main result of this work is the calculation of the fast ion distribution function $f(\rho, v_{||}, v_{\perp})$ for two different NBI lines and plasmas: perpendicular injection for LHD and tangential for TJ-II. Many relevant quantities can be estimated as moments of such distribution. The steady state profiles of toroidal and poloidal rotation and radial velocity are calculated in this way. The toroidal rotation velocity is the fraction of rotation provided by fast ions, which is important to estimate the NBI capability for rotation driving. The interest of the calculation of poloidal rotation relies particularly on its capability for creating shear flows, which could help to reduce the turbulence and to create transport barriers.

The slowing down time is also computed and compared with Spitzer's formula, showing the effect of the particular magnetic configuration and injection properties on that quantity. The slowing down time appears to be of the same order of the fast ion confinement time in the two studied cases, which means that the heating efficiency is negatively affected by the lost of ions. Comparison with experimental data [6, 7] measured with NPA's (Neutral Particle Analyzers) will be done in the near future. From the time evolution of f it is possible to estimate the momentum and energy transfer to the background plasma.

Acknowledgments

This work has been partially funded by the Spanish Ministerio de Ciencia e Innovacion, Spain, under Projects ENE2008-06082/FTN and FIS2009-12648-C03-0L. The computing resources used in these simulations have been provided by the EULER cluster at CIEMAT and by the Fusion Virtual Organization in the EGEE project.

References

[1] C. Alejaldre, J. J. Alonso, J. Botija, F. Castejón, J. R. Cepero, J. Guasp, A. Lopez-Fraguas, L. Garcia, V. I. Krivenski, R. Martín, A. Navarro, A. Perea, A. Rodriguez-Yunta, M. Sorolla, and A. Varias, *Fusion Technology* **17**, 131 (1990).

[2] F. Castejón, L. Fernández, J. Guasp, V. Martin-Mayor, A. Tarancón, and J. Velasco, *Plasma Physics and Controlled Fusion* **49**, 753 (2007).

[3] F. Castejón, J. Velasco, A. López-Fraguas, A. Tarancón, J. Guasp, F. Tabarés, M. Pedrosa, E. de la Cal, and M. Ochando, *Nuclear Fusion* **49**, 085019 (2009).

[4] S. Murakami, A. Fukuyama, T. Akutsu, N. Nakajima, V. Chan, M. Choi, S. Chiu, L. Lao, V. Kasilov, T. Mutoh, R. Kumazawa, T. Seki, K. Saito, T. Watari, M. Isobe, T. Saida, M. Osakabe, M. Sasao, and L. E. Group, *Nuclear Fusion* **46**, S425 (2006).

[5] T. H. Stix, *Plasma Physics* **14**, 367 (1971).

[6] M. Osakabe, S. Murakami, M. Yoshinuma, K. Ida, A. Whiteford, M. Goto, D. Kato, T. Kato, K. Nagaoka, T. Tokuzawa, Y. Takeiri, and O. Kaneko, *Review of Scientific Instruments* **79**, 10E519 (2008).

[7] R. Balbin, S. Petrov, J. Fontdecaba, K. McCarthy, V. Vargas, J. Carmona, J. Guasp, and D. Makarin, *EPS 2005 meeting, Tarragona, Spain, D5.001* (2005).